Asian Journal of Chemistry; Vol. 33, No. 1 (2021), 231-239

ASIAN JOURNAL OF CHEMISTRY

https://doi.org/10.14233/ajchem.2021.22966

Structural, Vibrational, Quantum Chemical Calculations, Thermal and Antimicrobial Studies on Sulphate Salt of 3-Nitroaniline

S. THANGARASU[1,*], V. SIVA[2], S. ASATH BAHADUR[2] and S. ATHIMOOLAM[3]

[1]Department of Physics, School of Advanced Sciences, Kalasalingam Academy of Research and Education, Krishnankoil-626126, India
[2]Condensed Matter Physics Laboratory, International Research Centre, Kalasalingam Academy of Research and Education, Krishnankoil-626126, India
[3]Department of Physics, Anna University, University College of Engineering, Nagercoil-629004, India

*Corresponding author: E-mail: sthangarasu@gmail.com

Received: 26 August 2020; *Accepted*: 12 November 2020; *Published online*: 10 December 2020; AJC-20203

In this work, *bis*(3-nitroanilinium) sulfate (3NASU) has been synthesized and crystallized successfully by solution growth combined with solvent evaporation technique. The studied salt, 3NASU molecular structure has been optimized with density functional theory (DFT) using B3LYP function and Hartree-Fock method with a 6-311++G(d,p) basis set. The geometrical parameters of 3NASU have been analyzed. The computed vibrational spectra were compared with experimental result which show appreciable agreement. Thermal stability of the crystal was analyzed with TGA/DTA and the melting points of the salt identified at 210 ºC. HOMO-LUMO energy calculations have shown the charge transfer within the molecule. The possible pharmaceutical/biological activity of the salts confirmed by the frontier molecular orbital (FMO) analysis have lower band gap value. The antimicrobial activity of grown crystals were tested against certain potentially threatening microbes.

Keywords: 3-Nitroaniline, Crystal structure, DFT, Vibrational assignments, HOMO-LUMO, Antimicrobial activity.

INTRODUCTION

Generally nitroaniline is called as push-pull molecule. Because of the intramolecular charge transfer (ICT) from the $–NH_2$ (electron-donor group) to $–NO_2$ (electron-acceptor group) through the phenyl ring. 3-Nitroaniline and 4-nitroaniline are used as reference compounds for optical nonlinearity [1-3] calculated by computational and experimental method. 3-Nitroaniline and its derivatives are biologically important compounds, such compounds are produced significant antihyperglycemic as well as hypoglycemic effects in alloxan-induced and normal diabetic rabbits [4]. Also *m*-nitroaniline plays an essential role in several biological processes and has considerable chemical and pharmacological importance. Since a long time, Schiff base compounds are generally considered due to their importance in several electro-optical and other biological applications [5].

In the recent decade has observed many developments in the design and characterization of the single crystals with the pharmacological importance. Based on literature survey it has acknowledged that biological, medicinal, industrial, pharmacological and agricultural applications compounds are belongs to methyl, nitro, chloro substituted benzaldehyde and Schiff bases [6,7]. These Schiff base compounds obtained from aromatic amines and aromatic aldehydes have a shown number of applications in many fields including chemical science, life sciences and pharmaceutical including analytical and inorganic chemistry [8]. Crystalline host compounds have a great deal of interest in the field of crystal engineering and supramolecular chemistry due to their practical and fundamental applications in magnetism, electro and non-linear optics and drug delivery [9].

In this context, a new family of organic-inorganic crystals with the biological importance, with chemical, physical and thermal properties through inorganic sub networks is proposed. Based on the above specifics, 3-nitroaniline was reacted with sulphuric acid and the crystals of *bis*(3-nitroanilinium)sulphate were grown. In this paper, the synthesis, crystal growth, structural, spectroscopic, thermal analyses and biological activity of *bis*(3-nitroanilinium) sulfate is reported.

EXPERIMENTAL

Bis(3-nitroanilinium)sulfate (3NASU) was synthesized fromAR grade 3-nitroaniline and sulphuric acid obtained from Himedia fine Chemicals taken in the 2:1 ratio from acetone. The chemicals were dissolved in acetone and stirred well using a magnetic stirrer for about 1 h (Fig. 1) at room temperature. The purity of the synthesized compound was improved by repeated re-crystallization process with acetone.

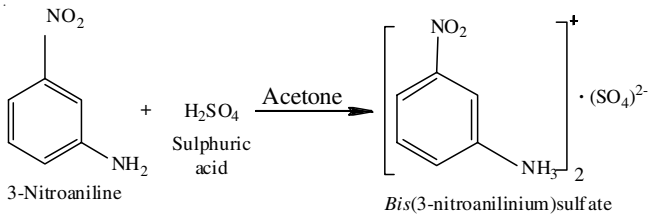

Fig. 1. Reaction scheme of *bis*(3-nitroanilinium)sulfate (3NASU)

Density measurements: The density of the grown crystals was determined by the floatation method using a liquid mixture of xylene and carbon tetrachloride. Initially, carbon tetrachloride (5 mL) was taken in a test tube and any one of the good-quality crystals was placed on it. The crystal began to float due to high density of the liquid. To get uniform density over the liquid, drops of xylene were added drop by drop using micropipette with continuous agitation. When the density of crystal matches that of liquid mixture, the crystal levitates to the middle of test tube. Finally, density of the liquid was found with specigravity bottle from the concept of relative density. Thus, the densities of the crystals are found to be 1.587 Mg m^{-3} for 3NASU.

Unit cell determination: The unit cell parameters were determined from single-crystal XRD data obtained with a Bruker SMART APEX CCD area detector diffractometer (graphite-monochromated, $MoK_\alpha = 0.71073$ Å). The data collection and cell refinement were made using SAINT program [11]. Further, the obtained crystal data parameters are presented in Table-1 in comparison with the reported literature values.

Characterization techniques: FT-IR spectrum of grown crystal was recorded using Nexus 670 FTIR spectrometer and FT-Raman spectrum were recorded using BRUKER RFS 27 FT-Raman spectrometer. Both the spectra were recorded in the range of 4000 to 400 cm^{-1} with Nd:YAG laser at 1064 nm as source. DTA/TGA of grown crystals were carried out by SII (SEIKO), Japan Analytical Instrument and Model No: TG/DTA-6200 with N_2 atmosphere with heating rate 20 °C/min.

TABLE-1
UNIT CELL PARAMETERS OF 3NASU

Crystal data	3NASU [Ref. 10]	3NASU
Unit cell dimensions	a = 7.9177 (16) Å b = 30.843 (6) Å c = 6.3924 (13) Å	a = 7.9172(16) Å b = 30.838(6) Å c = 6.3919(13) Å
Volume (V)	1561.1 (5) $Å^3$	1560.58 (2) $Å^3$
Density (ρ)	1.585 $Mg.m^{-3}$	1.587 $Mg.m^{-3}$
Crystal system, space group	Orthorhombic, Pbcm	Orthorhombic, Pbcm

Computational profile: The Hartree–Fock (HF) method and density functional theory (DFT) are used to carry out the efficient quantum mechanical calculations to optimize the molecular structure with 6-311++G(d,p) basis set using Gaussian 09W [12] program package on an Intel Core i5/3.20 GHz computer, raised gradient geometry optimization [13]. HF and DFT method [14] calculation used for the computation of molecular structure and vibrational frequencies with the three-parameter hybrid function (B3) [15] for the exchange part and the Lee-Yang-Parr (LYP) correlation function [16]. The GAUSSVIEW program [17] with symmetry considerations is used to make the vibrational frequency assignments with a high degree of accuracy. The electronic properties, such as HOMO-LUMO energies were calculated and computed by the HF and DFT method.

RESULTS AND DISCUSSION

Structural and molecular geometry analyses: The asymmetric part of unit cell contains 3-nitroaniline cation and the charge neutrality is attained with the sulphate anion in 3NASU. The optimized bond length and bond angles of 3NASU are presented in the Table-2. The optimized structure of *bis*(3-nitroanilinium) sulphate diagram and atom numbering scheme are shown in the Fig. 2.

The optimized C-C bond lengths are around 1.377-1.416 Å at HF method and 1.389-1.420 Å at B3LYP method, which well matches with the experimental results [18]. The single S–O bond is observed to be 1.544 Å. The corresponding optimized bond length is 1.548 Å at HF method and 1.598-1.599 Å at B3LYP method. The double S=O bond is observed to be 1.43 Å. The corresponding optimized bond length is 1.412 Å at HF method and 1.452 Å at B3LYP method.

Mulliken charge analysis: The histogram of atomic charges of 3NASU was shown in Fig. 3 and the computed charge values were given in Table-3. The hydrogen atoms in sulphate group have more electropositive (H17 and H34), because this hydrogen atom enclosed by electronegative oxygen atoms (O3 and O4)

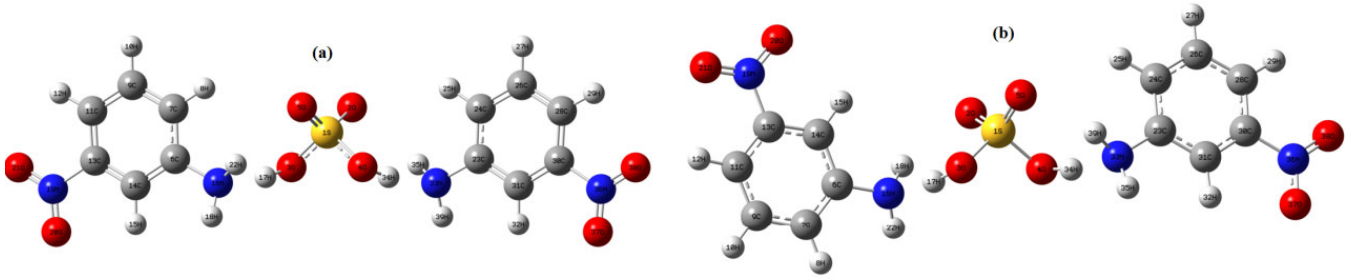

Fig. 2. Optimized geometry of *bis*(3-nitroanilinium)sulfate (3NASU) by (a) HF and B3LYP (b) method

TABLE-2
OPTIMIZED MOLECULAR GEOMETRICAL PARAMETERS OF 3NASU

Geometrical parameters	Experimental values	HF/6-311++G(d,p)	B3LYP/6-311++G(d,p)
Bond length (Å)			
S1–O3	1.452 (3)	1.548	1.599
S1–O4	1.471 (2)	1.548	1.598
S1–O5	1.449 (3)	1.412	1.452
C6–C7	1.373 (2)	1.391	1.400
C6–C14	1.385 (2)	1.384	1.396
C7–C9	1.378 (3)	1.382	1.392
C9–C11	1.380 (2)	1.386	1.392
C11–C13	1.379 (2)	1.378	1.390
C13–C14	1.376 (3)	1.382	1.389
C6–N16	1.451 (3)	1.416	1.420
C13–N19	1.473 (3)	1.469	1.484
N19–O20	1.201 (2)	1.188	1.224
N19–O21	1.211 (2)	1.186	1.224
Bond angle (°)			
O3–S1–O4	110.9 (1)	103.0	103.1
O3–S1–O5	110.4 (1)	108.7	106.7
O4–S1–O5	108.8 (1)	106.8	108.6
C7–C6–N16	119.9 (1)	120.0	120.4
C14–C6–N16	118.7 (1)	120.4	120.0
C11–C13–N19	119.2 (1)	118.9	118.8
C14–C13–N19	117.8 (1)	118.1	118.3
C7–C6–C14	121.3 (1)	119.6	119.5
C6–C7–C9	119.9 (1)	120.3	120.5
C7–C9–C11	120.4 (1)	120.9	120.7
C9–C11–C13	118.2 (1)	117.6	117.8
C11–C13–C14	122.9 (1)	122.9	122.9
C6–C14–C13	117.2 (1)	118.7	118.6
C13–N19–O20	118.7 (1)	117.6	117.6
C13–N19–O21	117.7 (1)	117.6	117.5
O20–N19–O21	123.6 (1)	124.8	124.8

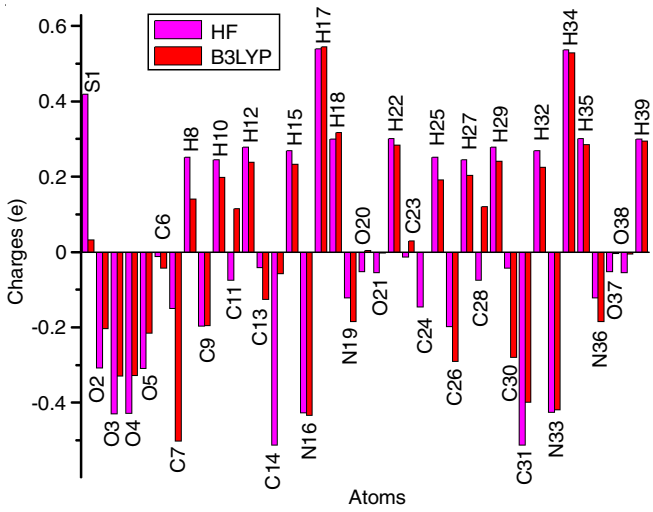

Fig. 3. Histogram of atomic charges on 3NASU by HF and B3LYP methods

and nitrogen atoms (N16 and N31). Also, this hydrogen atom was participated in N-H···O intermolecular hydrogen bond interactions in crystalline state [19]. Also, carbon atom has more electro negativity (C14 and C31), because this atom was enclosed by two electronegative carbon atoms and one hydrogen atom.

TABLE-3
COMPUTED ATOMIC CHARGES OF 3NASU

Atoms connected	HF/6-311++G(d,p)	B3LYP/6-311++G(d,p)
S1	0.418	0.031
O2	-0.309	-0.204
O3	-0.430	-0.330
O4	-0.428	-0.328
O5	-0.309	-0.216
C6	-0.012	-0.043
C7	-0.150	-0.502
H8	0.251	0.140
C9	-0.197	-0.196
H10	0.244	0.197
C11	-0.076	0.114
H12	0.277	0.238
C13	-0.042	-0.127
C14	-0.513	-0.058
H15	0.268	0.233
N16	-0.428	-0.434
H17	0.539	0.544
H18	0.299	0.316
N19	-0.122	-0.185
O20	-0.053	0.004
O21	-0.055	-0.004
H22	0.300	0.283
C23	-0.014	0.028
C24	-0.147	0.000
H25	0.250	0.191
C26	-0.198	-0.291
H27	0.244	0.203
C28	-0.076	0.120
H29	0.277	0.240
C30	-0.043	-0.280
C31	-0.513	-0.399
H32	0.268	0.224
N33	-0.427	-0.420
H34	0.536	0.529
H35	0.300	0.285
N36	-0.122	-0.185
O37	-0.053	-0.005
O38	-0.055	-0.005
H39	0.299	0.294

Vibrational analysis: The 3NASU consists of 39 atoms, which has 111 modes of vibrations. The comparison of experimental and computed IR and Raman spectra of 3NASU are given in Fig. 4 and frequency values are given in Table-4.

NH_2 vibrations: In NH_2 group vibrations are classified into six types of antisymmetric stretching, symmetric stretching, scissoring, twisting, wagging and rocking modes. The NH_2 antisymmetric stretching vibration [20,21] is scaled at 3826 & 3825 cm^{-1} in HF and 3590 & 3586 cm^{-1} in B3LYP method (mode 111 and mode 110). Similarly, NH_2 symmetric stretching vibration is calculated at 3738 & 3737 cm^{-1} in HF and 3494 & 3487 cm^{-1} in B3LYP method (mode 109 and mode 108). NH_2 scissoring vibration is calculated by HF and B3LYP method in the range of 1835-1655 cm^{-1} (mode 97, mode 96, mode 95 and mode 94). NH_2 twisting vibration is computed at 1626 cm^{-1} in HF and 1491 cm^{-1} in B3LYP method (mode 86). The NH_2 wagging vibrations is calculated at 1050 and 971 cm^{-1} in HF and B3LYP method (mode 61), respectively. These vibrations peaks are not observed in experimental spectra. The

TABLE-4
EXPERIMENTAL (FT-IR, FT-RAMAN) AND CALCULATED FREQUENCIES OF 3NASU WITH THEIR VIBRATIONAL ASSIGNMENTS

Mode number	Observed frequency (cm^{-1})		Calculated frequency (cm^{-1})						Vibrational assignments
			HF			B3LYP			
	IR	Raman	ν_{cal}	$^{a}I^{IR}$	$^{b}I^{Raman}$	ν_{cal}	$^{a}I^{IR}$	$^{b}I^{Raman}$	
1			7	0.649	0.034	6	0.763	0.1166	Lattice vibration
2			8	1.327	0.552	10	1.325	0.0649	Lattice vibration
3			16	1.058	0.182	16	1.352	0.9521	Lattice vibration
4			24	0.976	3.357	18	2.783	0.2723	Lattice vibration
5			28	8.031	0.803	23	2.052	1.7339	Lattice vibration
6			31	2.942	3.329	32	0.911	8.2586	Lattice vibration
7			36	3.295	0.355	33	3.956	2.3294	Lattice vibration
8			39	0.179	0.239	44	0.160	0.5947	$t(NO_2)$
9			40	0.098	1.006	47	0.565	0.2906	$t(NO_2)$
10			68	1.635	0.941	67	0.255	0.5232	β(S–OH)
11			81	3.377	1.683	91	2.421	3.0763	β(C–C)
12			95	13.227	0.087	110	19.111	0.1588	β(C–C)
13			143	45.307	1.525	152	44.453	0.7781	β(C–H)
14			147	1.257	1.411	156	5.015	2.0017	γ(C–H)
15			192	8.070	1.855	177	41.659	1.5108	γ(C–H)
16			192	3.212	3.504	182	12.492	4.488	γ(C–H)
17			239	0.020	0.610	219	1.704	0.791	$\rho(NH_2 + NO_2)$
18			239	5.333	0.684	222	1.967	0.6756	$\rho(NH_2 + NO_2)$
19			275	10.773	0.334	266	47.617	0.4661	γ(C–H + C–C)
20			276	3.870	0.333	269	20.151	0.6883	$\omega(NH_2)$
21			387	7.460	2.380	354	0.010	1.2423	γ(S–OH)
22			394	16.518	0.081	368	5.124	1.4823	$\rho(NH_2 + NO_2)$
23			417	0.235	4.747	370	2.883	3.106	$\rho(NH_2 + NO_2)$
24			423	1.181	4.604	384	0.204	7.1975	$t(NH_2)$ + β(S–OH)
25			425	0.833	0.905	397	2.745	2.9117	$\rho(NH_2)$
26			441	0.246	3.494	403	0.375	5.0234	$\rho(NH_2)$
27			461	17.353	0.044	430	2.084	0.7724	γ(C–H)
28			470	0.368	0.166	433	1.338	0.0323	γ(C–H)
29			475	7.307	0.043	455	36.895	1.731	$\rho(NH_2)$
30			492	9.346	2.749	482	12.386	3.2768	$\rho(NH_2)$
31			553	1.986	1.778	514	18.186	5.3827	γ(C–C + C–H)
32	507 m		554	0.643	7.831	519	16.940	1.1122	$t(NH_2)$
33			584	3.296	0.672	523	26.089	3.2501	$\delta(SO_4$ of $H_2SO_4)$
34			587	0.549	1.676	526	27.828	5.0437	γ(N–H)
35			590	28.872	0.973	532	27.074	1.8238	γ(C–H + C–C)
36			605	5.990	1.346	547	1.359	2.0658	β(C–C) + $t(NH_2)$
37			606	4.432	0.970	552	30.848	1.4017	β(C–C) + $t(NH_2)$
38			610	36.088	2.244	563	1.139	1.5964	β(C–C) + $\rho(NO_2 + NH_2)$
39	645 m		620	136.504	2.175	566	6.644	0.9699	β(C–C) + $t(NH_2)$
40			727	12.253	0.349	676	26.659	0.3589	γ(C–H)
41	679 w		727	46.855	0.130	677	28.463	0.3121	γ(C–H)
42			739	3.157	0.027	687	1.578	3.913	β(C–C)
43			739	3.742	10.662	689	4.967	4.7557	β(C–C)
44			807	34.338	0.250	730	13.484	1.0199	γ(C–H + NO_2)
45			810	17.221	1.549	731	13.152	1.5257	γ(C–H + NO_2)
46	715 w		834	22.036	0.395	800	68.620	27.3665	ν_s(S–OH of H_2SO_4)
47			838	39.735	2.008	802	174.357	5.8475	γ(C–H)
48			899	59.067	1.474	805	60.963	2.1467	γ(C–H)
49			900	5.800	2.532	815	465.568	0.775	γ(C–H)
50	806 w	806 w	905	331.488	0.498	823	9.592	20.6409	$\delta(NO_2)$ + β(C–C) + ν(C–N)
51			907	1.983	14.049	849	301.177	0.7534	$\omega(NH_2)$ + γ(C–H)
52			964	32.057	32.023	862	31.482	30.5257	$\omega(NH_2)$ + γ(C–H)
53			978	359.152	1.861	878	103.948	2.6163	$\omega(NH_2)$ + γ(C–H)
54			984	71.686	8.836	912	34.086	0.5295	γ(C–H)
55		1002 w	1014	417.912	1.182	921	47.901	0.6769	γ(C–H)
56			1019	45.136	3.254	929	26.487	0.9071	γ(C–H)

57			1029	385.157	4.228	938	12.378	3.737	γ(C–H + S–OH)
58	1013 w		1033	131.074	0.379	943	32.794	1.425	γ(C–H)
59			1034	7.369	12.737	945	22.545	2.0568	γ(S–OH) + β(C–H)
60			1050	9.550	5.694	948	457.275	29.8522	ω(NH_2) + γ(S–OH)
61			1050	23.491	2.339	971	322.484	58.7022	ω(NH_2) + γ(S–OH)
62			1084	11.112	5.463	996	0.801	0.3094	γ(C–H)
63			1084	2.588	60.445	1005	1.374	2.2773	γ(C–H)
64			1115	2.689	0.181	1015	3.000	31.6655	β(C–C)
65			1115	0.586	0.100	1016	4.589	34.7078	β(C–C)
66			1158	3.820	1.912	1095	19.408	0.4758	ρ(NH_2)
67	1152 sh		1159	0.891	2.239	1097	17.429	0.9735	ρ(NH_2)
68			1205	5.755	3.074	1105	25.363	19.3906	β(C–C + C–H) + ν(C–N)
69			1206	64.544	4.218	1106	22.036	19.5293	β(C–C + C–H) + ν(C–N)
70			1214	14.754	0.678	1129	170.772	40.1711	ν(SO_4 of H_2SO_4)
71			1214	7.814	17.226	1152	4.422	4.3695	t(NH_2)
72			1268	0.771	0.824	1155	1.622	1.9764	t(NH_2) + β(C–C + C–H)
73			1269	7.272	3.948	1191	0.525	2.1003	β(C–H)
74			1285	205.944	14.425	1194	1.651	3.2282	β(C–H)
75	1347 s	1359 s	1351	22.376	5.804	1264	82.709	36.7099	β(C–C + C–H) + ν(C–N)
76			1351	1.488	1.482	1267	30.503	66.4214	β(C–C + C–H) + ν(C–N)
77			1366	88.641	2.348	1282	290.278	2.34	β(S–OH)
78			1367	37.158	46.012	1331	35.491	1.5461	β(C–H)
79			1391	184.648	0.771	1331	7.862	8.5499	β(C–H)
80			1422	42.040	3.497	1364	23.687	0.4443	ν(C–C)
81			1446	13.817	0.223	1366	39.449	14.1296	ν(C–C)
82			1448	1.429	1.543	1371	300.320	175.6911	ν_s(NO_2) + ν(C–N)
83			1538	422.952	0.672	1372	232.297	168.591	ν_s(NO_2) + ν(C–N)
84			1614	95.290	1.021	1389	47.623	6.6403	β(S–OH)
85			1614	57.509	30.338	1441	136.636	0.9624	β(S–OH)
86			1626	419.087	20.326	1491	2.877	2.4184	ν(C–C) + t(NH_2)
87			1626	119.662	138.607	1494	1.687	3.6103	ν(C–C) + t(NH_2)
88			1647	2.026	2.671	1516	64.922	0.161	ν(C–C) + ν(N–O)
89			1647	11.965	17.027	1516	13.962	0.6061	ν(C–C)
90	1531 s		1770	244.707	5.285	1588	383.685	26.5612	ν_{as}(NO_2)
91			1770	371.298	40.727	1592	359.998	24.8705	ν_{as}(NO_2)
92	1612 sh		1782	115.556	69.062	1631	22.232	57.8832	ν(C–C)
93			1782	96.892	3.743	1633	19.013	65.7048	ν(C–C)
94			1803	242.987	20.169	1655	28.310	4.1918	δ(NH_2)
95			1803	173.850	2.631	1660	7.839	9.7986	δ(NH_2)
96			1835	49.690	5.114	1665	52.444	15.1138	δ(NH_2)
97			1835	260.473	2.292	1669	66.540	13.2926	δ(NH_2)
98	2866 sh		3339	2.421	49.781	2909	5379.794	101.5697	ν(O–H)
99			3339	3.776	69.336	2960	552.153	1009.353	ν(O–H)
100	3062 br	3085 w	3356	3.171	96.495	3167	6.305	71.5322	ν(C–H)
101			3356	4.049	123.603	3178	1.796	72.2926	ν(C–H)
102			3380	5.667	33.882	3192	5.324	148.6871	ν(C–H)
103			3380	4.631	57.449	3195	2.861	120.1103	ν(C–H)
104			3401	3.676	73.116	3207	4.615	51.2483	ν(C–H)
105			3401	3.471	75.341	3208	7.346	46.5291	ν(C–H)
106			3611	3324.392	34.049	3230	3.621	87.0077	ν(C–H)
107			3635	142.551	468.442	3231	4.169	88.4235	ν(C–H)
108			3737	87.053	52.775	3487	81.985	152.828	ν_s(NH_2)
109			3738	34.627	129.589	3494	54.349	166.1284	ν_s(NH_2)
110			3825	30.402	32.704	3586	34.489	48.5638	ν_{as}(NH_2)
111			3826	34.842	35.292	3590	35.225	40.81	ν_{as}(NH_2)

ν, Stretching; w-weak; m- medium; vs - very strong;
γ- out-of- plane bending; β- in-plane bending; ν_s, sym. stretching; ν_{as}, asym.stretching; ρ -rocking; δ - scissoring; t- twisting; ω-wagging.

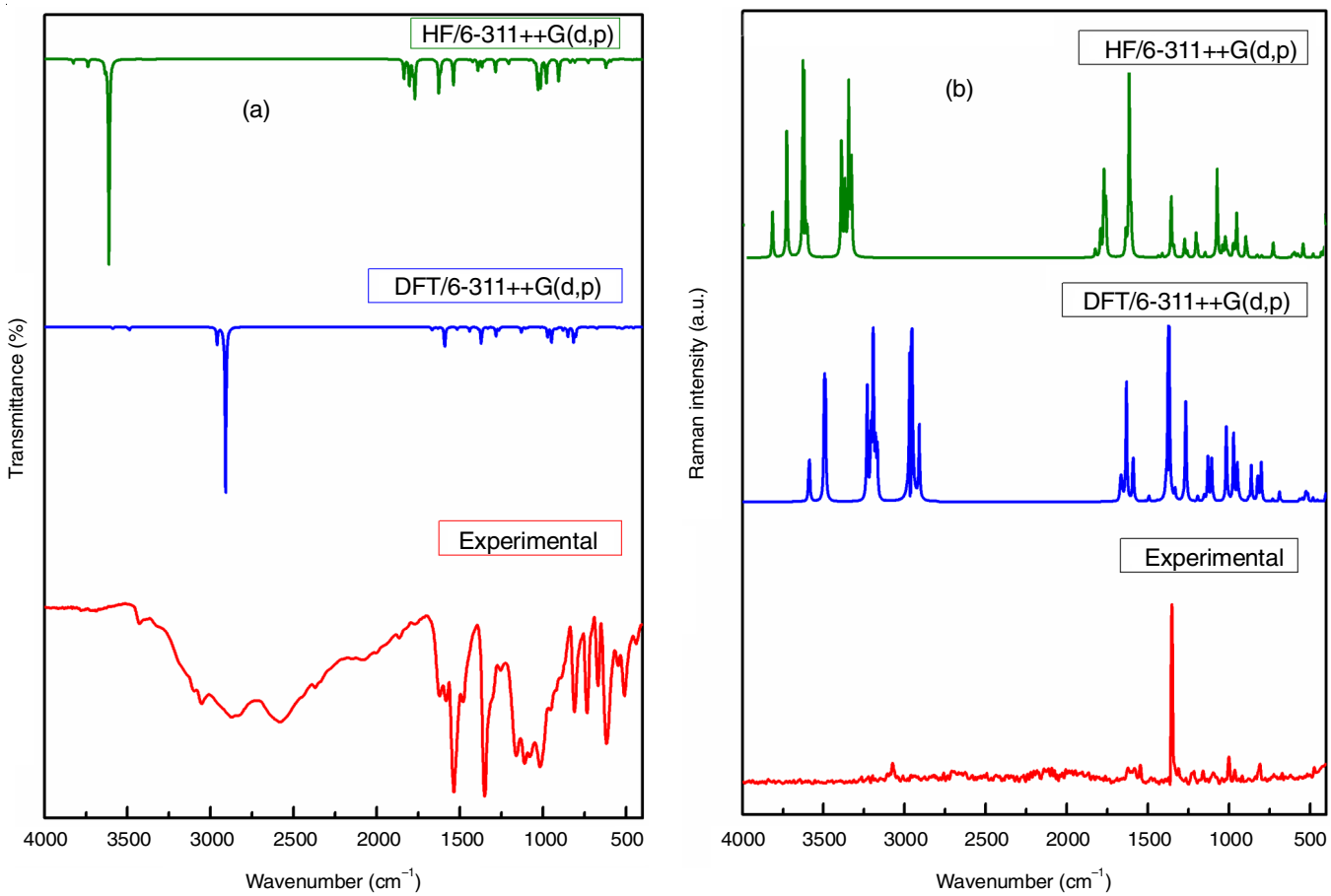

Fig. 4. Experimental and computed IR & Raman spectra of *bis*(3-nitroanilinium)sulfate (3NASU)

NH_2 rocking vibrations observed as a shoulder peak in Raman and scaled at 1159 and 1097 cm^{-1} in HF and B3LYP method (mode 67), respectively.

NO_2 vibrations: The NO_2 group asymmetric stretching vibrations are observed in the region around 1500-1570 cm^{-1} and NO_2 group symmetric stretching [22] vibrations are observed in the region around 1370-1300 cm^{-1} in nitrobenzene and substituted nitrobenzene compounds. The NO_2 asymmetric stretching vibrations observed as a strong peak at 1531 cm^{-1} in IR and theoretically computed at 1770 & 1770 cm^{-1} in HF and 1588 & 1592 cm^{-1} in B3LYP method (mode 91, mode 90). The NO_2 symmetric stretching vibrations are theoretically scaled at 1538 and 1448 cm^{-1} in HF and 1372 & 1371 cm^{-1} in B3LYP method (mode 83, mode 82). The NO_2 scissoring vibrations observed as a weak peak at 806 cm^{-1} in IR and Raman. The corresponding calculated wavenumbers at 905 cm^{-1} in HF and 823 cm^{-1} in B3LYP method (mode 50). The NO_2 rocking vibrations are calculated at 610 and 563 cm^{-1} in HF and B3LYP method (mode 38), respectively.

C–C and C–N vibrations: The C–C and C–N stretching vibrations appears in 1600–1300 cm^{-1} region. The shoulder peak at 1612 cm^{-1} assigned to C–C stretching vibrations and it is computed at 1782 and 1631 cm^{-1} in HF and B3LYP method (mode 92), respectively. The same stretching vibrations are computed by the theoretical calculations by HF and B3LYP method at mode 93, mode 92, mode 89, mode 88, mode 87 & mode 86. The C–N stretching vibrations calculated at 1538 and 1372 cm^{-1} in HF and B3LYP method (mode 83), respectively.

C-H vibrations: The aromatic structure of the title compound represent by C–H stretching vibrations, it occurs in the characteristic region around 3100 cm^{-1}. Hence a broad band observed at 3062 cm^{-1} in IR and a weak peak assigned at 3085 cm^{-1} in Raman is assigned for C–H stretching vibration [23,24]. The same stretching vibrations are theoretically calculated by HF and B3LYP method at mode 107 to mode 100 in the range of 3635-3167 cm^{-1}. The band around of 1300-1100 cm^{-1} and 1100-900 cm^{-1} represents aromatic C–H in-plane bending and out-plane bending vibrations, respectively. For the title compound C–H in-plane bending vibration calculated wavenumbers at 1367 and 1331 by HF and B3LYP method (mode 78), respectively. The C–H out-plane bending vibration theoretically calculated at 1084 cm^{-1} in HF and 1055 cm^{-1} in B3LYP method (mode 63).

Vibrations of sulfate group: The sulfate anion plays a vital role in forming hydrogen bonds with the cation and stabilizing the crystal structure. In sulfate anion, the O–H stretching mode is observed as a shoulder peak at 2866 cm^{-1} in IR and it is theoretically scaled at 3339 & 3339 cm^{-1} in HF and 2960 & 2909 cm^{-1} in B3LYP method (mode 99 & mode 98). The corresponding band in Raman is absent. The stretching mode of SO_4 group expected to occur in the region 1100-1050

cm^{-1}. It is scaled at 1214 and 1129 cm^{-1}. in HF and B3LYP method (mode 70), respectively. The scissoring mode of SO_4 group is scaled at 584 cm^{-1} in HF and 523 in B3LYP method (mode 33). For the above corresponding vibrations observed peaks are absent in IR and Raman. The in plane bending vibrations of S–OH is calculated in the mode 85 & mode 84 by HF and B3LYP method in the range of 1614–1389 cm^{-1}. The out plane bending vibrations of S–OH is calculated in the mode 61 & mode 60 by HF and B3LYP method in the range of 1050–948 cm^{-1}.

Frontier moleculer orbital analysis: In the organic molecules, optical and electric properties are proposed by using frontier molecular orbital analysis. The molecular orbital have two important interactions; such as HOMO means the ability to donate an electron and LUMO represents accept an electron. Also, these orbitals are named as frontier orbitals. Frontier electron density [25] is used to explain the several types of reaction in conjugated system and most reactive position in π-electron systems. Also, FMO plays an essential part in abiding chemical stability of the compound [26]. The calculated HOMO and LUMO energies and some important parameters of the 3NASU were calculated by HF and DFT/B3LYP method as shown in Table-5. The stimulated energy level diagrams of 3NASU molecule was shown in Fig. 5. A huge amount of charge transfer occurred in 3NASU is indicated by small energy gap, which is connected with a high chemical reactivity. The small value of energy gap and high value of charge transfer leads the molecules to biologically active.

For 3NASU, 654 energy levels are observed in the energy ranges of -92.276 to 192.615 a.u. and -0.891 to 189.248 a.u. in HF and DFT/B3LYP method, respectively. The calculated HOMO and LUMO energy values of 3NASU molecule in HF and B3LYP level are -0.356/0.026 and -0.269/-0.112 a.u. The energy gap value between the frontier orbital was 0.382 a.u in HF and 0.157 a.u in B3LYP level.

TABLE-5
CALCULATED ENERGY VALUES OF 3NASU

Parameters (a.u.)	HF/6-311++G(d,p)	B3LYP/6-311++G(d,p)
E_{LUMO}	0.026	-0.112
E_{HOMO}	-0.356	-0.269
$\delta(E_{LUMO} - E_{HOMO})$	0.382	0.157
Electron affinity (A)	-0.026	0.112
Ionization potential (I)	0.356	0.269
Chemical hardness (η)	0.191	0.079
Chemical potential (?)	-0.165	-0.191
Electronegativity (χ)	0.165	0.191
Electrophilicity index	0.071	0.231

Thermal analysis: The thermal behaviour of 3NASU was studied using simultaneous DTA/TGA analysis with temperature range around 40-750 °C. The DTA/TGA curves of 3NASU were shown in the Fig. 6. The DTA/TGA curve represent that the decomposition is in the range of 210-750 °C. The decomposition of 3NASU occurs in three main steps and it is shown in Fig. 7. The first stage of decomposition in the temperature range of 180-210 °C with weight loss 5% due to the loss of water molecule from the title compound. The second stage of decomposition and major weight loss 46% occurred in the temperature range around 210-250 °C. It is due to loss of NO, CO_2 and SO_2 from former compound. The last stage of decomposition is occurred in the temperature range of 250-380°C with weight loss 31% owing to removal of C_2H_4 and NO. Carbon and nitrogen mixture may be final residue. The endothermic weak peak observed at 112.3 °C is due to the removal of lattice water molecule. A second endothermic peak observed at 210 °C is due to the melting point of the title compound. An exothermic peak at 268.2 °C is owing to the decomposition of the organic compound.

Antimicrobial activity analysis: To analyze the antimicrobial activity of 3NASU, the crystal was tested against

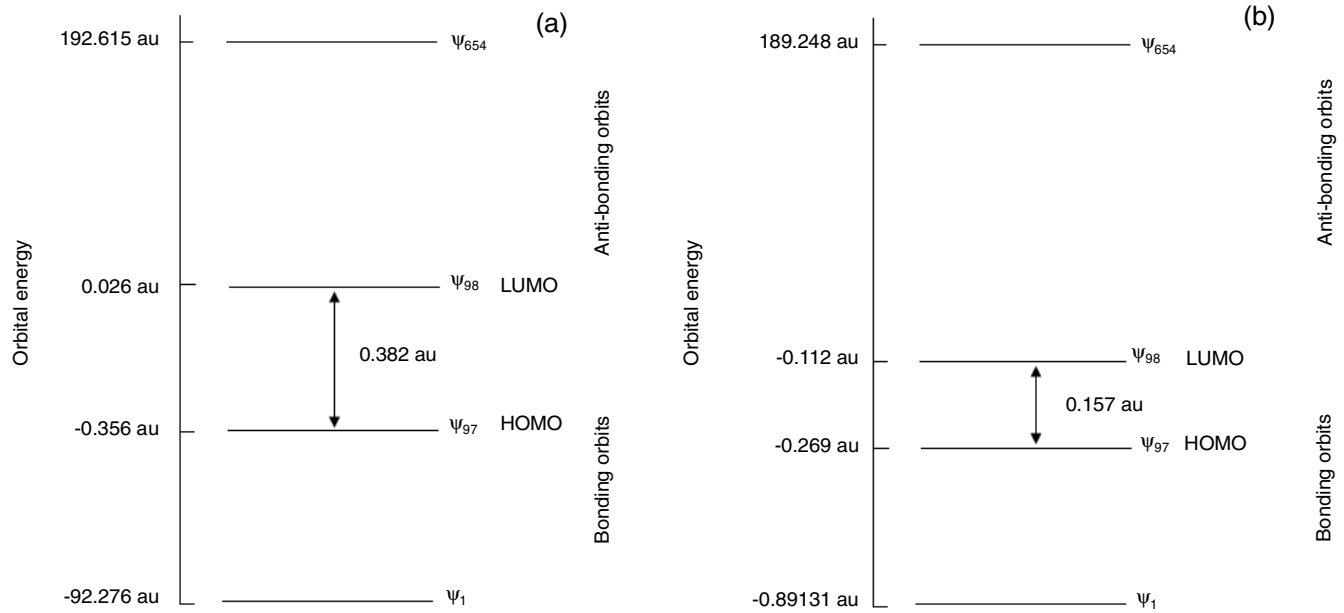

Fig. 5. Molecular orbital energy level diagram of *bis*(3-nitroanilinium)sulfate (3NASU) by (a) HF and (b) B3LYP levels

TABLE-6
ANTIBACTERIAL AND ANTIFUNGAL ACTIVITY OF 3NASU COMPOUND AGAINST SOME HUMAN PATHOGENS

Sample	Concentration (mg/mL)	Zone of inhibition in diameter (mm)		
		Gram-positive: *K. neumoniae*	Gram-negative: *S. aureus*	*C. albicans*
3NASU	50	10	R	10
	100	10	R	10
SD	50/100	16	18	16

R = Resistant; SD-Standard drug (antibacterial activity)–Amikacin; SD-Standard drug (antifungal activity)–Ketokonazole

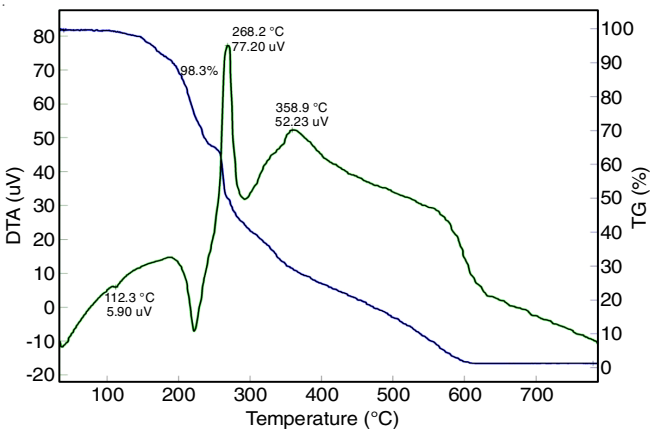

Fig. 6. DTA/TGA curve of 3NASU

Step-I

$C_{12}H_{14}N_4O_8S$ (374) $\xrightarrow{180–210\ °C}$ $C_{12}H_{12}N_4O_7S$ (356) + H_2O (18)

Step-II

$C_{12}H_{12}N_4O_7S$ (356) $\xrightarrow{210–250\ °C}$ $C_{11}H_{12}N_2O$ (188) + 2NO (60) + CO_2 (44) + SO_2 (64)

Step-III

$C_{11}H_{12}N_2O$ (188) $\xrightarrow{250–380\ °C}$ C_5N (74) + $3C_2H_4$ (84) + NO (30)

Note: The values given in parenthesis stand for the molecular weights of the respective species.

Fig. 7. Decomposition steps of 3NASU

Staphylococcus aureus (Gram-positive) and *Klebsiella pneumoniae* (Gram-negative) by disc diffusion method with 50 and 100 mg mL^{-1} concentrations [27]. Similarly, the antifungal activity of 3NASU was tested against *Candida albicans* [28]. The zone of inhibition were measured in diameter and its values are shown in Table-6. The biological activity of *bis*(3-nitroanilinium)sulfate complex results indicate, it is a moderately active material against all the organisms.

Conclusion

Bis(3-nitroanilinium) sulfate was synthesized and characterized. The detailed interpretation of the vibrational spectra between calculated (IR, Raman) and computed spectra, experimental results of *bis*(3-nitroanilinium)sulfate (3NASU) molecule show the good reliability with computed results. The higher stability of the title molecule is confirmed from the computed HOMO-LUMO energy gap. TGA and DTA exposed about the material, thermal analysis confirmed the absence of phase transition before the material reach the melting point. Antimicrobial activity of the title compound has been calculated.

CONFLICT OF INTEREST

The authors declare that there is no conflict of interests regarding the publication of this article.

REFERENCES

1. V. Krishnakumar and R. Nagalakshmi, *Cryst. Growth Des.*, **8**, 3882 (2008); https://doi.org/10.1021/cg070548i
2. D.M. Bishop, B. Champagne and B. Kirtman, *J. Chem. Phys.*, **109**, 9987 (1998); https://doi.org/10.1063/1.477665
3. H. Reis, M.G. Papadopoulos, P. Calaminici, K. Jug and A.M. Köster, *Chem. Phys.*, **261**, 359 (2000); https://doi.org/10.1016/S0301-0104(00)00305-0
4. A.K. Jain, S.C. Mehta and N.M. Shrivastava, *Indian J. Pharm.*, **37**, 395 (2005); https://doi.org/10.4103/0253-7613.19078
5. V. Siva, A. Shameem, A. Murugan, S. Athimoolam, M. Suresh and S.A. Bahadur, *Chem. Data Coll.*, **24**, 100281 (2019); https://doi.org/10.1016/j.cdc.2019.100281
6. P. Anand, V.M. Patil, V.K. Sharma, R.L. Khosa and N. Masand, *Int. J. Drug Des. Discov.*, **3**, 851 (2012).
7. N. Aggarwal, R. Kumar, P. Dureja and D.S. Rawat, *J. Agric. Food Chem.*, **57**, 8520 (2009); https://doi.org/10.1021/jf902035w
8. V. Patel, P. Trivedi, H. Gohel and D. Khetani, *Int. J. Adv. Pharm. Biol. Chem.*, **3**, 999 (2014).
9. V.S.V. Satyanarayana, P. Sreevani, A. Sivakumar and V. Vijayakumar, *ARKIVOC*, 221 (2008); https://doi.org/10.3998/ark.5550190.0009.h21
10. L. Feng, Y. Hou, X. Yong and F. Bao, *Acta Crystallogr. Sect. E Struct. Rep. Online*, **65**, o1086 (2009); https://doi.org/10.1107/S1600536809013762
11. SAINT Bruker, SMART, Brucker AXS Inc., Madison, Wisconsin (2001).
12. M.J. Frisch, G.W. Trucks, H.B. Schlegel, G.E. Scuseria, M.A. Robb, J.R. Cheeseman, J.A. Montgomery Jr., T. Vreven, K.N. Kudin, J.C. Burant, J.M. Millam, S.S. Iyengar, J. Tomasi, V. Barone, B. Mennucci, M. Cossi, G. Scalmani, N. Rega, G.A. Petersson, H. Nakatsuji, M. Hada, M. Ehara, K. Toyota, R. Fukuda, J. Hasegawa, M. Ishida, T. Nakajima, Y. Honda, O. Kitao, H. Nakai, M. Klene, X. Li, J.E. Knox, H.P. Hratchian, J.B. Cross, V. Bakken, C. Adamo, J. Jaramillo, R. Gomperts, R.E. Stratmann, O. Yazyev, A.J. Austin, C. Cammi, J.W. Pomelli, P.Y. Ochterski, K. Ayala, G.A. Morokuma, P. Voth, R. Salvador, J.J. Dannenberg, V.G. Zakrzewski, S. Dapprich, A.D. Daniels, M.C. Strain, O. Farkas, D.K. Malick, A.D. Rabuck, K. Raghavachari, J.B. Foresman, J.V. Ortiz, Q. Cui, A.G. Baboul, S. Clifford, J. Cioslowski, B.B. Stefanov, G. Liu, A. Liashenko, P. Piskorz, I. Komaromi, R.L. Martin, D.J. Fox, T. Keith, M.A. AlLaham, C.Y. Peng, A. Nanayakkara, M. Challacombe, P.M.W. Gill, B. Johnson, W. Chen, M.W. Wong, C. Gonzalez and J.A. Pople, Gaussian Inc., Wallingford, CT (2009).
13. R.G. Parr and W. Yang, Density-Functional Theory of Atoms and Molecules, Oxford University Press (1989).
14. W. Koch and M.C. Holthausen, A Chemist's Guide to Density Functional Theory, Wiley-VCH: Weinheim (2000).
15. D. Young, Computational Chemistry: A Practical Guide for Applying Techniques to Real World Situations, Wiley-Interscience (2001).
16. H.B. Schlegel, *J. Comput. Chem.*, **3**, 214 (1982); https://doi.org/10.1002/jcc.540030212

17. R. Dennington, T. Keith and J. Millam, Gauss View, Version 5.0.8 Semichem Inc., Shawnee Mission KS (2013).
18. S. Thangarasu, S. Athimoolam and S.A. Bahadur, *Acta Crystallogr. Sect. E Struct. Rep. Online*, **67**, o2124 (2011); https://doi.org/10.1107/S1600536811029072
19. S. Thangarasu, V. Siva, S. Athimoolam and S.A. Bahadur, *J. Theor. Comput. Chem.*, **17**, 1850021 (2018); https://doi.org/10.1142/S0219633618500219
20. M. Suresh, V. Siva, S.A. Bahadur and S. Athimoolam, *J. Mol. Struct.*, **1221**, 128820 (2020); https://doi.org/10.1016/j.molstruc.2020.128820
21. A. Anandhan, C. Sivasankari, M. Saravanabhavan, V. Siva and K. Senthil, *J. Mol. Struct.*, **1203**, 127400 (2020); https://doi.org/10.1016/j.molstruc.2019.127400
22. S. Premkumar, A. Jawahar, T. Mathavan, M.K. Dhas, V.G. Sathe and A.M.F. Benial, *Spectrochim. Acta Mol. Biomol. Spectrosc.*, **129**, 74 (2014); https://doi.org/10.1016/j.saa.2014.02.147
23. N. Bhuvaneswari, N. Priyadharsini, S. Sivakumar, K. Venkatachalam and V. Siva, *J. Therm. Anal. Calorim.*, **136**, 411 (2019); https://doi.org/10.1007/s10973-018-7908-1
24. V. Siva, S.S. Kumar, M. Suresh, M. Raja, S. Athimoolam and S.A. Bahadur, *J. Mol. Struct.*, **1133**, 163 (2017); https://doi.org/10.1016/j.molstruc.2016.11.088
25. N. Prabavathi, A. Nilufer and V. Krishnakumar, *Spectrochim. Acta A Mol. Biomol. Spectrosc.*, **114**, 449 (2013); https://doi.org/10.1016/j.saa.2013.05.011
26. V. Krishnakumar, N. Jayamani, R. Mathammal, *J. Raman Spectrosc.*, **40**, 936 (2009); https://doi.org/10.1002/jrs.2203
27. M. Ahamad, R.M. Rao, M.M. Rafi, G.J. Mohinddin and J. Sreeramulu, *Arch. Appl. Res.*, **4**, 858 (2012).
28. K.D. Park, J.H. Lee, S.H. Kim, T.H. Kang, J.S. Moon and S.U. Kim, *Bioorg. Med. Chem. Lett.*, **16**, 3913 (2006); https://doi.org/10.1016/j.bmcl.2006.05.033